Large deflection analysis of orthotropic, elliptic membranes

Somchai Chucheepsakul[†]

Department of Civil Engineering, King Mongkut's University of Technology Thonburi,
Bangmod, Tungkru, Bangkok 10140, Thailand

Sakdirat Kaewunruen[‡]

RailCorp - Track Engineering, Level 13, 477 Pitt St., Sydney, NSW 2000, Australia

Apiwat Suwanarat[‡†]

Department of Civil Engineering, King Mongkut's University of Technology Thonburi,
Bangmod, Tungkru, Bangkok 10140, Thailand

Abstract. Applications of membrane mechanisms are widely found in nano-devices and nano-sensor technologies nowadays. An alternative approach for large deflection analysis of the orthotropic, elliptic membranes – subject to gravitational, uniform pressures often found in nano-sensors – is described in this paper. The material properties of membranes are assumed to be orthogonally isotropic and linearly elastic, while the principal directions of elasticity are parallel to the coordinate axes. Formulating the potential energy functional of the orthotropic, elliptic membranes involves the strain energy that is attributed to in-plane stress resultant and the potential energy due to applied pressures. In the solution method, Rayleigh-Ritz method can be used successfully to minimize the resulting total potential energy generated. The set of equilibrium equations was solved subsequently by Newton-Raphson. The unparalleled model formulation capable of analyzing the large deflections of both circular and elliptic membranes is verified by making numerical comparisons with existing results of circular membranes as well as finite element solutions. The results are found in excellent agreements at all cases. Then, the parametric investigations are given to delineate the impacts of the aspect ratios and orthotropic elasticity on large static tensions and deformations of the orthotropic, elliptic membranes.

Keywords: membrane structures; elliptic membranes; circular membranes; nonlinear static analysis; large deflections; large static tension; Rayleigh-Ritz method; energy minimization.

† Professor, Ph.D., Corresponding author, E-mail: somchai.chu@kmutt.ac.th
‡ Senior Engineer, Ph.D., E-mail: sakdirat@hotmail.com
‡† Former Research Associate

1. Introduction

Nano-technology draws much incentive from a huge number of researchers and scholars in diverse fields in recent years. One of the applications used in nano-technology is the membrane. Generally membranes are very emaciated with the 1000-8000 nm ($\times 10^{-9}$ m) in depth. Although almost of membrane applications lay on physics and nano-science, there are a number of civil engineering applications of structural membranes such as the pneumatic structures in long span fabrics, and inflatable shells in roof structures. In addition, the pressure sensors in electronic micro/ nano chips, coating films resisting the dynamic abrasion, corrosion, chemical attack, or any-substance permeation in mechanical elements, beams, girders, etc., and landing and magnetic balloons in modern spacecraft, or even cell tissues and textures are some of apparent applications of membrane mechanism.

A brief overview of literatures related to membrane problems in the twentieth century is presented. Hencky (1915) developed the stress propagation model for circular membranes under pressures in polar coordinates. Tayler's series was employed to assume the deflection and stress functions, made up of the unknown parameters and membrane radius. However, the recent finding shows that the accuracy of Hencky's model is impaired slightly unless the series is kept 12 terms at most (Fitcher 1997). After 1970s, there existed some investigations about membrane probes. Kao and Perrone (1972) applied Hencky model to flat arbitrary membranes. Finite difference method was embroiled in the numerical computation for static equilibrium solutions. Analogously, Storåkers (1983) studied Hencky model via shooting optimization method. Galerkin and Rayleigh-Ritz methods were used to scrutinize the orthotropic rectangular membranes by Kondo and Uemura (1972). Since the modern applications of membranes are of substantially small pieces (nano-size), therefore the accuracy and precision of the model for predicting the membrane behaviors is necessary. A system that meets the need is *"Micro-Electo Mechanical Systems (MEMS),"* which has been developed for the electronic pressure sensors. This system has been investigated by Voothuyzen and Berveld (1984) and Sheplak and Dugundji (1998). From most of the literature, it can be indicated that the preceding membrane research tasks only deal with isotropic materials, and membranes of circular shape. They mostly exploit simply polar coordinates, thereby resulting in their convenient analyses of just these limited types. This can not be applied to all situations. Recently, there are a number of studies on membrane structures. The majority of these studies imposed finite elements in the static analyses (Wu *et al.* 1996, Bonet 2000, Bouzidi *et al.* 2003). Bouzidi and Le van (2004) reported that traditional finite element theory had troublesome procedures. They then developed a numerical approach for analyzing hyperelastic circular and rectangular membranes, and proved that their method using Newton method in energy minimization could be well used in such analyses. However, the procedures of such approach are still complicated and limited to a circle shape of curved membranes. Simultaneously, to enhance the capacity of various-shape membrane analysis, the present study is an endeavor that implements the alternative approach on the basis of energy method. An additional aim is at being practicable to all elliptic, circular or strip membranes.

In this study, the total potential energy of membranes includes strain energy that is ascribed to axial stretching and virtual work due to uniform load burdens. Material properties of the membranes studied are assumed orthogonally isotropic and of elliptic profiles. Bending rigidity and their own weight are neglected. The membranes are considered irresistible to compressions and obey Hooke's law. Lessening the convergence of results, finite element method becomes inexpedient for meshing

the elements because of the membrane appearance. Compared to FEM, Rayleigh-Ritz method is therefore judged more apt to treat the mesh functional for the stiffness matrix, hence leading to a more accurate solution. The simplicity and practicality of this computer method could also attract a large number of researchers or engineers in related fields, particularly in nano-membranes or nano-textiles.

2. Variational formulations

The nonlinear static equilibrium configuration is determined by considering the uniform pressures distributed over the membrane. After facing the external forces, the membrane will deform − with large deflections − from the initial position to static equilibrium configuration due to the symmetrical burden. Fig. 1 portrays the typical geometry of elliptic membranes and Fig. 2 depicts the member forces in an element of the membranes.
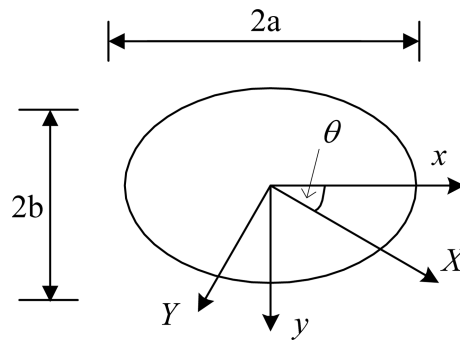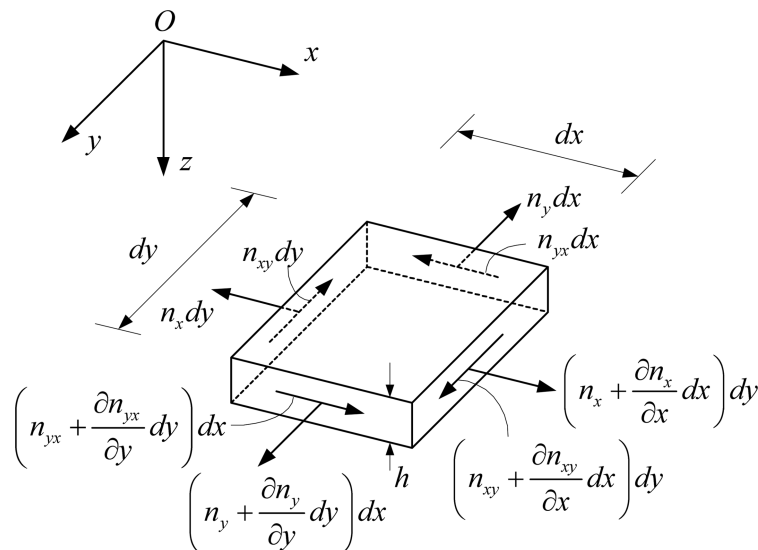

Fig. 1 Typical geometry of elliptic membranes

Fig. 2 Resulting forces in a membrane element

2.1 Strain energy

In this case, the strain energy due to bending is neglected since the membrane has a very emaciated depth, comparative to the width and the length of all of the membranes. Analogously, the out-of-plane transverse-shear strain remains less and is then ignored. Thus, the axial strain due to in-plane stress resultants (planar tensions) becomes significant and is expressed as follows.

$$U_m = \frac{1}{2}\iint_A (n_x \varepsilon_x + n_y \varepsilon_y + n_{xy}\gamma_{xy})dxdy \tag{1}$$

where, $\varepsilon_x, \varepsilon_y, \gamma_{xy}$ represent the axial strains in x and y directions, and the transverse-shear strain in x-y plane. The tensions in x and y directions and the transverse shear force in x-y plane are in terms of n_x, n_y, n_{xy}, respectively.

Arranged dimensionless, Eq. (1) turns to

$$U_m = \frac{1}{2}abE_x h\iint_A (\hat{n}_x \varepsilon_x + n_y \varepsilon_y + n_{xy}\gamma_{xy})d\xi d\eta \tag{2}$$

The lengths of membranes in x and y directions are communicated by a and b; vice versa, h stands for the constantly uniform depth of membranes; E_x for the modulus of elasticity, conforming to the principal elastic axis, X; ξ and η for non-dimensional coordinates (x/a, y/b); and, $\hat{n}_x, \hat{n}_y$, and $\hat{n}_{xy}$ for non-dimensional tensions ($n_x/E_x h, n_y/E_x h$, and $n_{xy}/E_x h$), respectively.

Hooke's law is applied to the stress-strain relation, considering the membrane property as an orthotropic material. The non-dimensional matrix form of the relation reads

$$\begin{Bmatrix} \hat{n}_x \\ \hat{n}_y \\ \hat{n}_{xy} \end{Bmatrix} = \frac{1}{(1-\nu_X\nu_Y)}\begin{bmatrix} 1 & \hat{C}_{12} & C_{13} \\ \hat{C}_{21} & C_{22} & C_{23} \\ \hat{C}_{31} & C_{32} & C_{33} \end{bmatrix}\begin{Bmatrix} \varepsilon_x \\ \varepsilon_y \\ \gamma_{xy} \end{Bmatrix} \tag{3}$$

The constants, $\hat{C}_{ij}$, stand for

$$C_{11} = A_{11}\cos^4\theta + A_{22}\sin^4\theta + 2(A_{12}+2A_{33})\cos^2\theta\sin^2\theta$$

$$\hat{C}_{12} = C_{21} = \frac{[A_{12}+[A_{12}+A_{22}-2(A_{12}+2A_{33})]\cos^2\theta\sin^2\theta]}{C_{11}}$$

$$\hat{C}_{13} = C_{31} = \frac{[A_{11}\cos^3\theta\sin\theta - A_{22}\cos\theta\sin^3\theta - (A_{12}+2A_{33})(\cos^2\theta-\sin^2\theta)\cos\theta\sin\theta]}{C_{11}}$$

$$\hat{C}_{22} = \frac{[A_{11}\sin^4\theta + A_{22}\cos^4\theta + 2(A_{12}+2A_{33})\cos^2\theta\sin^2\theta]}{C_{11}} \tag{4}$$

$$\hat{C}_{23} = C_{32} = \frac{[A_{11}\cos\theta\sin^3\theta - A_{22}\cos^3\theta\sin\theta + (A_{12}+2A_{33})(\cos^2\theta-\sin^2\theta)\cos\theta\sin\theta]}{C_{11}}$$

$$\hat{C}_{33} = \frac{[A_{33}+[A_{11}+A_{22}-2(A_{12}+2A_{33})]\cos^2\theta\sin^2\theta]}{C_{11}}$$

and

$$A_{11} = \frac{E_X}{(1 - v_X v_Y)}$$

$$A_{22} = \frac{E_Y}{(1 - v_X v_Y)}$$

$$A_{33} = G_{XY}$$

$$A_{12} = \frac{v_X E_Y}{(1 - v_X v_Y)} = \frac{v_Y E_X}{(1 - v_X v_Y)}$$

where; E_X and E_Y are moduli of elasticity with respect to the principal elastic axes, X and Y respectively; G_{XY} is the shear modulus in x-y plane; and, v_X and v_Y are the poisson's ratios in x and y directions.

Considering a case in which the principal elastic axes are parallel to the coordinate axes (x-y in Cartesian coordinates), θ that represents the angle between those 2 coordination systems approaches nil so that the Eq. (3) becomes

$$\begin{Bmatrix} \hat{n}_x \\ \hat{n}_y \\ \hat{n}_{xy} \end{Bmatrix} = \frac{1}{(1 - v_X v_Y)} \begin{bmatrix} 1 & v_X & 0 \\ v_X & \dfrac{E_Y}{E_X} & 0 \\ 0 & 0 & \dfrac{(1 - v_X v_Y)G_{XY}}{E_X} \end{bmatrix} \begin{Bmatrix} \varepsilon_x \\ \varepsilon_y \\ \gamma_{xy} \end{Bmatrix} \tag{5}$$

In Lagrangian coordinates with large-deflection theory, the strain-deformation relation can be written as follows.

$$\varepsilon_x = \frac{\partial u}{\partial x} + \frac{1}{2}\left(\frac{\partial w}{\partial x}\right)^2 \tag{6a}$$

$$\varepsilon_y = \frac{\partial v}{\partial y} + \frac{1}{2}\left(\frac{\partial w}{\partial y}\right)^2 \tag{6b}$$

$$\gamma_{xy} = \frac{\partial u}{\partial y} + \frac{\partial v}{\partial x} + \frac{\partial w}{\partial x}\frac{\partial w}{\partial y} \tag{6c}$$

where u, v, and w are the displacements in x, y, and z direction respectively.

Non-dimensional forms of the Eq. (6) are

$$\varepsilon_x = \frac{\partial \hat{u}}{\partial \xi} + \frac{1}{2}\left(\frac{\partial w}{\partial \xi}\right)^2 \tag{7a}$$

$$\varepsilon_y = \lambda\frac{\partial \hat{v}}{\partial \eta} + \frac{\lambda^2}{2}\left(\frac{\partial w}{\partial \eta}\right)^2 \tag{7b}$$

$$\gamma_{xy} = \lambda\frac{\partial \hat{u}}{\partial \eta} + \frac{\partial v}{\partial \xi} + \lambda\frac{\partial \hat{w}}{\partial \xi}\frac{\partial w}{\partial \eta} \tag{7c}$$

where $\hat{u}, \hat{v}$, and $\hat{w}$ represent the dimensionless displacements in x, y, and z direction (u/a, v/a, w/a) respectively. Also, λ stands for the major/minor radius ratio (a/b).

Replacing Eqs. (5) and (7) into Eq. (2) yields the following strain energy of membranes.

$$U_m = \frac{abE_x h}{2(1-v_x v_y)} \iint_A \left\{ \begin{array}{l} \left[\frac{\partial \hat{u}}{\partial \xi}+\frac{1}{2}\left(\frac{\partial w}{\partial \xi}\right)^2\right]^2 \\[2mm] +2v_x\left[\frac{\partial \hat{u}}{\partial \xi}+\frac{1}{2}\left(\frac{\partial w}{\partial \xi}\right)^2\right]\left[\lambda\frac{\partial \hat{v}}{\partial \eta}+\frac{\lambda^2}{2}\left(\frac{\partial w}{\partial \eta}\right)^2\right] \\[2mm] +\frac{E_y}{E_x}\left[\lambda\frac{\partial \hat{v}}{\partial \eta}+\frac{\lambda^2}{2}\left(\frac{\partial w}{\partial \eta}\right)^2\right]^2 \\[2mm] +\frac{(1-v_x v_y)G_{xy}}{E_x}\left[\lambda\frac{\partial \hat{u}}{\partial \eta}+\frac{\partial v}{\partial \xi}+\lambda\frac{\partial \hat{w}}{\partial \xi}\frac{\partial w}{\partial \eta}\right]^2 \end{array} \right\} d\xi d\eta \tag{8}$$

2.2 Potential energy of distributed load

The potential energy of uniformly distributed pressure $q(x,y)$ can be presented by

$$\Omega = -\iint_A q(x,y)w\,dxdy \tag{9}$$

The Eq. (9) can be re-arranged in the non-dimensional form as follows.

$$\Omega = -abE_x h\iint_A \hat{q}w\,d\xi d\eta \tag{10}$$

2.3 Total potential energy

The total potential energy is derived from the summation of strain energy and potential energy of the uniformly distributed load. Its expression is as follows.

$$\pi = \frac{abE_x h}{2(1-v_x v_y)} \iint_A \left\{ \begin{array}{l} \left[\frac{\partial \hat{u}}{\partial \xi}+\frac{1}{2}\left(\frac{\partial w}{\partial \xi}\right)^2\right]^2 \\[2mm] +2v_x\left[\frac{\partial \hat{u}}{\partial \xi}+\frac{1}{2}\left(\frac{\partial w}{\partial \xi}\right)^2\right]\left[\lambda\frac{\partial \hat{v}}{\partial \eta}+\frac{\lambda^2}{2}\left(\frac{\partial w}{\partial \eta}\right)^2\right] \\[2mm] +\frac{E_y}{E_x}\left[\lambda\frac{\partial \hat{v}}{\partial \eta}+\frac{\lambda^2}{2}\left(\frac{\partial w}{\partial \eta}\right)^2\right]^2 \\[2mm] +\frac{(1-v_x v_y)G_{xy}}{E_x}\left[\lambda\frac{\partial \hat{u}}{\partial \eta}+\frac{\partial v}{\partial \xi}+\lambda\frac{\partial \hat{w}}{\partial \xi}\frac{\partial w}{\partial \eta}\right] \\[2mm] -2(1-v_x v_y)\hat{q}w^2 \end{array} \right\} d\xi d\eta \tag{11}$$

3. Rayleigh-ritz method

From Fig. 1 describing the geometry of a membrane, when the membrane is loaded, it deforms to the static equilibrium whose total potential energy deems to be at lowest point. This is identical to the energy principles in that the conservative systems stay in equilibrium when the total potential energy leaves the lowest value. The assumed arbitrary displacement fields in Rayleigh-Ritz method are

$$\hat{u} = \sum_{i=1}^{l} a_i f_i(\xi, \eta) \tag{12a}$$

$$\hat{v} = \sum_{i=1}^{m} b_i g_i(\xi, \eta) \tag{12b}$$

$$\hat{w} = \sum_{i=1}^{n} c_i h_i(\xi, \eta) \tag{12c}$$

where a_i, b_i, and c_i are unknown parameters; f_i, g_i, and h_i represent the admissible shape functions conforming to the membranes' compatibility equations and essential boundary conditions.

By the principle of stationary potential energy, minimization of the total potential energy function Π by differentiating Eq. (11) with respect to generalized coordinates a_i, b_i, and c_i brings out the governing differential equations of $\hat{u}, \hat{v}$, and $\hat{w}$ respectively.

$$\frac{\partial \pi}{\partial a_i} = 0, \quad i = 1, \ldots, l \tag{13a}$$

$$\frac{\partial \pi}{\partial b_i} = 0, \quad i = 1, \ldots, m \tag{13b}$$

$$\frac{\partial \pi}{\partial c_i} = 0, \quad i = 1, \ldots, n \tag{13c}$$

From the governing equations emerge $l + m + n$ nonlinear stiffness equations. Newton-Raphson procedure is thus utilized to treat numerically the nonlinear problem for determining unknown parameters a_i, b_i, and c_i. These parameters are then returned to place in Eqs. (12a), (12b), and (12c), resulting in the generic displacement functions of membranes.

3.1 Boundary conditions of membranes

In general, elliptic membranes with simple supports prohibit displacements in x, y, and z directions except rotational angles at edges. The forced boundary conditions of the membranes considered can be expressed as $\hat{u} = v = w = 0$ at supports; thereby, the generalized coincident displacement functions are presented as follows.

$$\hat{u} = (1 - \xi^2 - \eta^2) \sum_{m=0}^{\infty} \sum_{n=0}^{\infty} a_{mn} \xi^m \eta^n \tag{14a}$$

$$\hat{v} = (1 - \xi^2 - \eta^2) \sum_{m=0}^{\infty} \sum_{n=0}^{\infty} b_{mn} \xi^m \eta^n \tag{14b}$$

$$\hat{w} = (1 - \xi^2 - \eta^2) \sum_{m=0}^{\infty} \sum_{n=0}^{\infty} c_{mn} \xi^m \eta^n \tag{14c}$$

It is noticeable that simply the first parts of Eqs. (14a), (14b), and (14c) concur with the boundary conditions of the membranes. The remaining portions of the equations are 2-dimension polynomial series. Axisymmetry exists when applied pressures are constant, $q(x,y) = q_0$. Then the Eqs. (14a), (14b), and (14c), matching the axisymmetric deformations, become

$$\hat{u} = \xi(1 - \xi^2 - \eta^2) \sum_{m=0,2,4,\dots}^{\infty} \sum_{n=0,2,4,\dots}^{\infty} a_{mn} \xi^m \eta^n \tag{15a}$$

$$\hat{v} = \eta(1 - \xi^2 - \eta^2) \sum_{m=0,2,4,\dots}^{\infty} \sum_{n=0,2,4,\dots}^{\infty} b_{mn} \xi^m \eta^n \tag{15b}$$

$$\hat{w} = (1 - \xi^2 - \eta^2) \sum_{m=0,2,4,\dots}^{\infty} \sum_{n=0,2,4,\dots}^{\infty} c_{mn} \xi^m \eta^n \tag{15c}$$

As witnessed, the Eq. (15a) additionally includes ξ; the Eq. (15b) also has an extra η; and, the whole countable numbers (m and n) remain only even figures – all for compromising the boundary condition set.

Factors involved in solutions analyzed by Rayleigh-Ritz method are:

- The chosen functions must form the complete set function that must be satisfiable to the forced boundary conditions. Fig. 3 illustrates the number of terms in complete sets of polynomial function relations in two independent variables (ξ and η); for example, the quadratic polynomial function establishes the complete set if its formula comprises 3 terms: 1, ξ^2, and η^2. The convergence to exact solutions is seemingly enhanced if the chosen functions also meet the natural boundary conditions.
- The number of series terms influences both the accuracy and the time used alterably: the more series terms, the more the accuracy. However, it is more time consuming to compute more series terms.

To modify the equilibrium equations into Rayleigh-Ritz format, the total potential energy Π, Eq. (11), is replaced by the Eqs. (15a) and (15b). Minimization of the substitute equation in accordance with Eqs. (13a) and (13b) initiates the nonlinear algebraic equations. After having spatial integration on throughout the membrane area, the Newton-Raphson algorithm is focused in

$$1$$
$$\xi^2 \qquad \eta^2$$
$$\xi^4 \qquad \xi^2\eta^2 \qquad \eta^4$$
$$\xi^6 \qquad \xi^4\eta^2 \qquad \xi^2\eta^4 \qquad \eta^6$$
$$\xi^8 \qquad \xi^6\eta^2 \qquad \xi^4\eta^4 \qquad \xi^2\eta^6 \qquad \eta^8$$
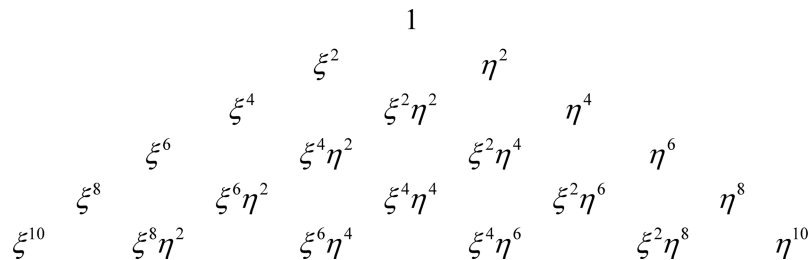$$\xi^{10} \qquad \xi^8\eta^2 \qquad \xi^6\eta^4 \qquad \xi^4\eta^6 \qquad \xi^2\eta^8 \qquad \eta^{10}$$

Fig. 3 Pascal triangle

order to carry out the undetermined constants of the algebraic equations. The displacement fields are thus completely defined and lead to nonlinear static solutions.

4. Results and disscussions

In this study, the result validation is made to confirm the correction of the mathematical model related to literatures dealing with circular membranes. Then, the parametric studies are done to divulge the impacts of Poisson's ratios, moduli of elasticity, and axis length ratios so-called aspect ratios ($\lambda = a/b$) on nonlinear static behaviors: internal forces, displacements.
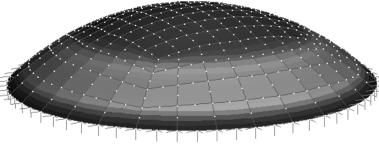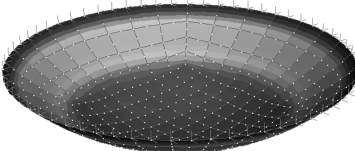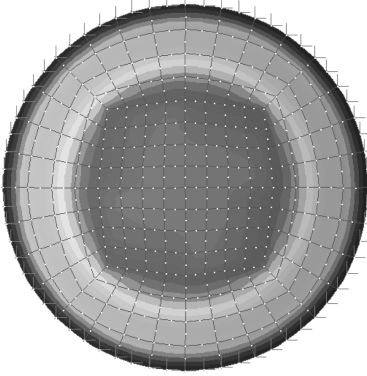
4.1 Result validation
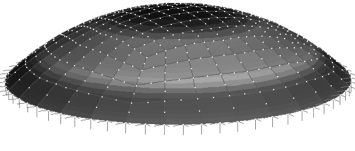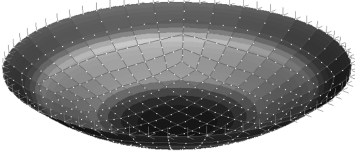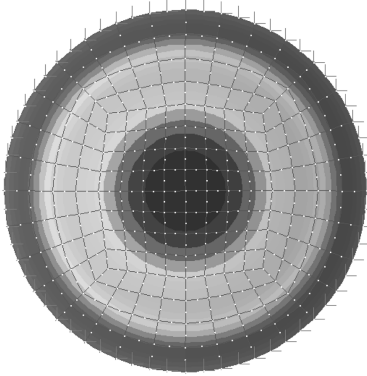
This model is modified to compare with the existing results of circular membranes (Hencky 1915, Fitcher 1997). The properties of membranes used in the verification are: $\lambda = 1$, $v_x = v_y = 0.3$, $E_y/E_x = 1$, and $G_{xy}/E_x = 0.385$. Varying the number of series' terms used, Table 1 shows the comparisons of results with solutions by series expansion (Hencky 1915) and by the shooting method (Fitcher 1997).

Table 1 shows that the results are in excellent agreement with those found in other reports. Although the 6×6×6-term element is ample to use in the scrutiny, the 10×10×10-term element is employed in this investigation, in order to get the strikingly accurate results that accompany well-fitting schedule. A finite element model of circular membrane has been developed using the nonlinear membrane elements in STRAND7 (2002). Table 2 depicts the nonlinear solutions of the circular membrane. Clearly, the Rayleigh-Ritz and finite element solutions are in very good agreement.

Table 1 Comparison of displacements and internal tensions at the center of circular membranes

| Number of terms in series | Displacements, $\hat{w}(0,0)$ | | | % Difference | |
	Fitcher (1997) by series expansions	Storåkers (1983) by shooting optimizations	This study by Rayleigh-Ritz	Fitcher (1997)	Storåkers (1983)
1 × 1 × 1	6.5345E-02	6.5300E-02	6.7924E-02	3.95	4.02
3 × 3 × 3	6.5345E-02	6.5300E-02	6.5141E-02	-0.31	-0.24
6 × 6 × 6	6.5345E-02	6.5300E-02	6.5359E-02	0.02	0.09
10 × 10 × 10	**6.5345E-02**	**6.5300E-02**	**6.5342E-02**	0.00	0.06
Number of terms in series	Internal tensions, $\hat{n}_x(0,0) = \hat{n}_y(0,0)$			% Difference	
	Fitcher (1997) by series expansions	Storåkers (1983) by shooting optimizations	This study by Rayleigh-Ritz	Fitcher (1997)	Storåkers (1983)
1 × 1 × 1	4.3110E-03	4.3103E-03	4.4525E-03	3.28	3.30
3 × 3 × 3	4.3110E-03	4.3103E-03	4.2707E-03	-0.93	-0.92
6 × 6 × 6	4.3110E-03	4.3103E-03	4.3237E-03	0.29	0.31
10 × 10 × 10	**4.3110E-03**	**4.3103E-03**	**4.3039E-03**	-0.16	-0.15

Table 2 Nonlinear finite element solutions of circular membranes

Contours	Isometric Views	Histograms

(m)

-0.003266

-0.016328

-0.022859

-0.035921

-0.042453

-0.055515

-0.065312

displacement
(0.05% difference from Rayleigh-Ritz)

(kN/m)

4.3186E-3

4.0594E-3

3.9557E-3

3.7484E-3

3.6447E-3

3.5410E-3

3.3337E-3

internal tension
(0.34% difference from Rayleigh-Ritz)

4.2 Parametric studies

Figs. 4 and 5 demonstrate the influence of aspect ratios (λ) on the displacements and internal tensions at the center of elliptic membranes. Based on the preliminary data of $\hat{q} = 0.001$, $v_x = v_y = 0.3$, $E_y/E_x = 1$, $G_{xy}/E_x = 0.385$, and varying λ from 0 to 2, it is found that the central displacement ($\hat{w}$) and internal x-direction tension ($\hat{n}_x$) change slightly at the interval of λ between 0 and 0.5. Moreover, they tend to be painstakingly reduced when λ values more than 0.5. Although the y-direction tension ($\hat{n}_y$) prevails the increment at the early λ and the highest tension takes place when λ reaches the value of 1.0, it tends to diminish after λ passes through 1.0.

Effects of Poisson's ratios (v) are illustrated in Figs. 6 and 7. Similarly, the data used in the study are alike as mentioned except varying the Poisson's ratios from 0 to 0.5. Apparently with the greater v, Fig. 6 marks that the central displacement ($\hat{w}$) tends to decrease. On the other hand, Fig. 7 signifies that the internal tensions ($\hat{n}_x$ and $\hat{n}_y$) tend to ascend particularly for the case that λ is
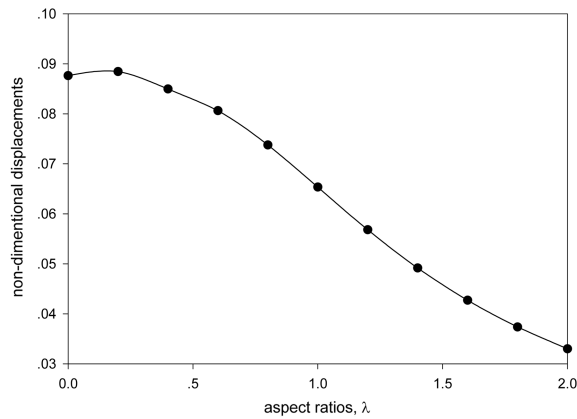

Fig. 4 Influence of aspect ratios (λ) on non-dimensional displacement ($\hat{w}$) at the center of elliptic membranes
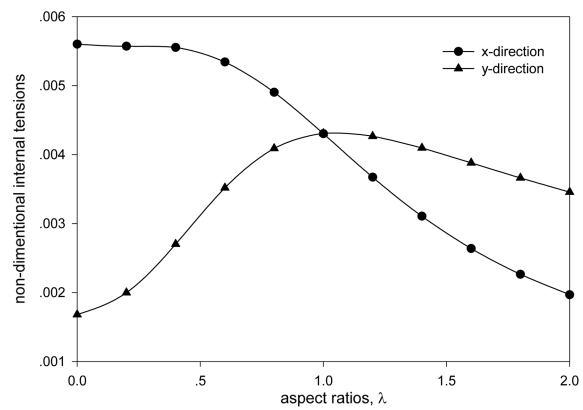
Fig. 5 Influence of aspect ratios (λ) on non-dimensional internal tensions ($\hat{n}_x$ and $\hat{n}_y$) at the center of elliptic membranes
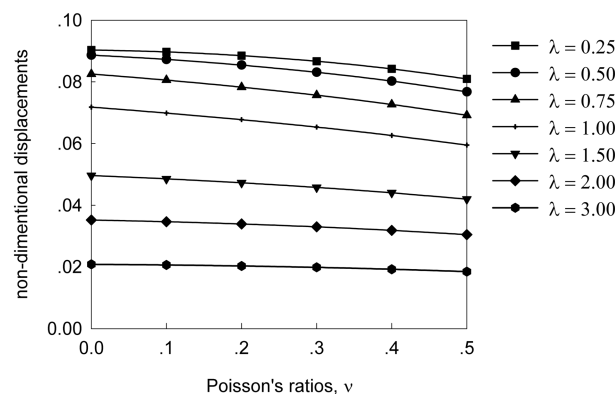

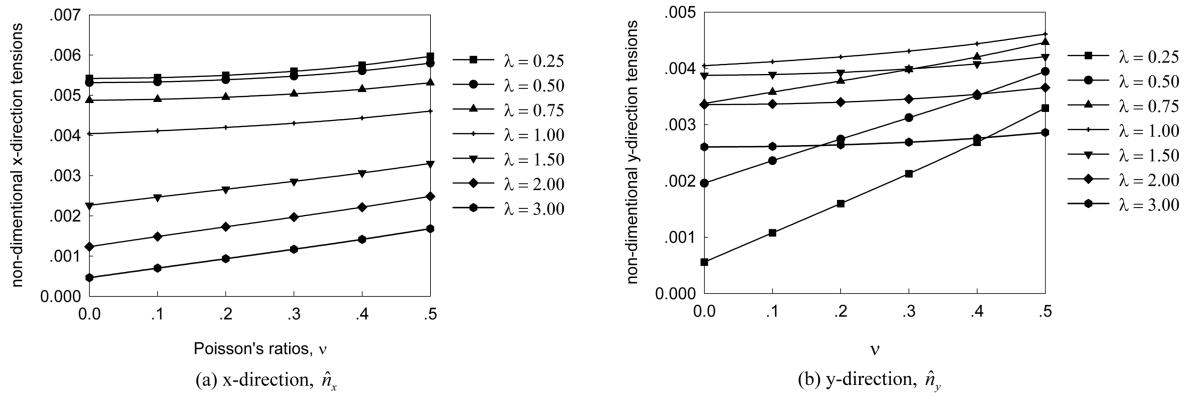Fig. 6 Influence of Poisson's ratios (v) on non-dimensional displacement ($\hat{w}$) at the center of elliptic membranes

(a) x-direction, $\hat{n}_x$ (b) y-direction, $\hat{n}_y$

Fig. 7 Influence of Poisson's ratios (ν) on non-dimensional internal tensions $(\hat{n}_x$ and $\hat{n}_y)$ at the center of elliptic membranes
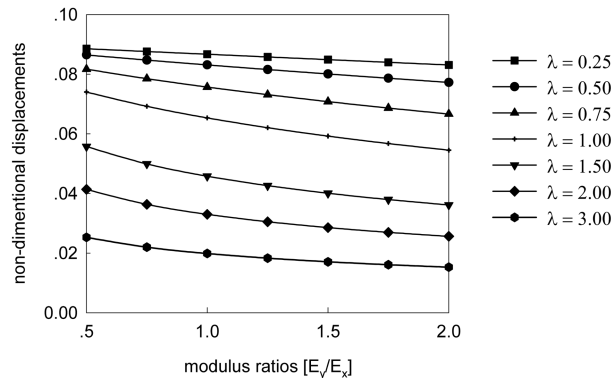

Fig. 8 Influence of modulus ratios (E_y/E_x) on non-dimensional displacement $(\hat{w})$ at the center of elliptic membranes
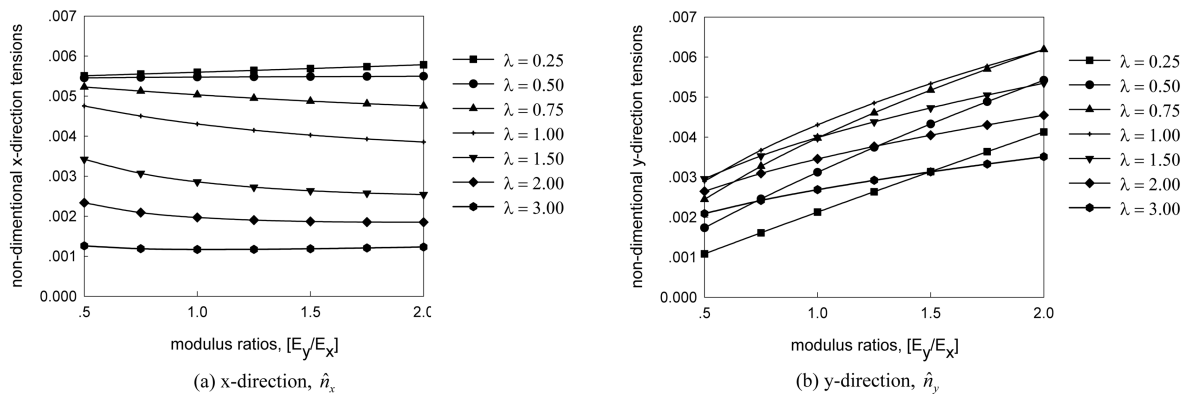

(a) x-direction, $\hat{n}_x$ (b) y-direction, $\hat{n}_y$

Fig. 9 Influence of modulus ratios (E_y/E_x) on non-dimensional internal tensions $(\hat{n}_x$ and $\hat{n}_y)$ at the center of elliptic membranes

equal to 0.5. Obviously the more λ, the lower $\hat{w}$, but also significantly lower tensions $(\hat{n}_x$ and $\hat{n}_y)$. These results indicate the importance of λ, in addition to that of Poisson's ratios, on displacements

and internal tensions at the center of membranes.

Ranging from 0.5 to 2.0, the modulus ratios (E_y/E_x) play role in the displacements and internal tensions of membranes as shown in Figs. 8 and 9. The decrement of the central displacement ($\hat{w}$) and the x-direction tension ($\hat{n}_x$) predominates while E_y/E_x ratios are higher. The manifest thriving of the y-direction tension ($\hat{n}_y$) implies the more E_y comparative to E_x. Likewise, λ meaningfully dominates the nonlinear static behaviors of the membranes.

5. Conclusions

Presented in this paper is an alternative approach, Rayleigh-Ritz method, for analyzing the large deflection behaviors of orthotropic elliptic membranes. By energy principles, the total potential energy is composed of the strain energies due to in-plane tensions and shear forces, and potential energy of the uniformly distributed burdens. Rayleigh-Ritz method subsequently takes considerable part in approximating displacement fields and Newton-Raphson algorithm then solves the algebraic set of nonlinear equilibrium equations by stationary potential energy, for static solutions. Excellent agreements of results make the mathematical model acceptable. Rayleigh-Ritz approximation fields are profoundly applicable to various shapes of membranes.

Parametric studies describe the impacts of aspect ratios (λ), Poisson's ratios (v), and modulus ratios (E_y/E_x) on the nonlinear static behaviors: displacements ($\hat{w}$) and internal tensions ($\hat{n}_x$ and $\hat{n}_y$), all at the center of membranes. Clearly, reduction of the displacements happens when aspect ratios, Poisson's ratios, and modulus ratios enlarge. Also, the greater λ induces the considerably lesser $\hat{n}_x$. The increasing v causes the gradually higher $\hat{n}_x$; however, the blooming E_y/E_x decreases the $\hat{n}_x$ by degrees. Even though $\hat{n}_y$ behaves like $\hat{n}_x$ in case of parameter v, its characteristic opposes the one of $\hat{n}_x$ in case of parameter E_y/E_x and varies in case of parameter λ. Besides, it can be concluded that the λ conspicuously predominates the effects of other parameters.

Acknowledgements

References

Bonet, J. (2000), "Finite element analysis of air supported membrane structures", *Comput. Meth. Appl. Mech. Eng.*, **190**, 579-595.

Bouzidi, R. and Le van, A. (2004), "Numerical solution of hyperelastic membranes by energy minimization", *Comput. Struct.*, **82**, 1961-1969.

Bouzidi, R., Ravaut, Y. and Wielgosz, C. (2003), "Finite elements for 2D problems of pressurized membranes", *Comput. Struct.*, **81**, 2479-2490.

Fitcher, W.B. (1997), "Some solutions for the large deflections of uniformly loaded circular membranes", NASA Technical Paper 3658. Hampton, Virginia, USA: NASA Langley Research Center, 1-20.

G+D Computing, Using STRAND7 Introduction to the Strand7 finite element analysis system (2002), Sydney G+D Computing Pty Ltd.

Hencky, H. (1915), "On the stress state in circular plates with vanishing bending stiffness", *Zeitschrift Für Mathematik und Physik*, **63**, 311-317.

Kao, R. and Perrone, N. (1972), "Large deflections of flat arbitrary membranes", *Comput. Struct.*, **2**, 535-546.

Kondo, K. and Uemura, M. (1972), "Deformations and stresses of orthotropic retangular membrane under uniform lateral pressure", *Proceedings of 1971 IASS Pacific Symposium Part II Tension Structures and Space Frames*, (2-7), 211-222.

Sheplak, M. and Dugundji, J. (1998), "Large deflections of clamped circular plates under initial tension and transitions to membrane behavior", *ASME J. Appl. Mech.*, **65**, 107-115.

Storåkers, B. (1983), "Small deflection of linear elastic circular membranes under lateral pressure", *ASME J. Appl. Mech.*, **50**, 735-739.

Voorthuyzen, J.A. and Bergveld, P. (1984), "The influence of tensile forces on the deflection of circular diaphragms in pressure sensors", *Sensor Actuat. A*, **6**, 201-213.

Wu, B., Du, X. and Tan, H. (1996), "A three-dimensional Fe nonlinear analysis of membranes", *Comput. Struct.*, **59**, 601-605.